



September 10 - 12, 2007

Pilsen, Czech Republic

# NUMERICAL MODELING OF THE INHOMOGENEITY IN MATERIALS

ING. EVA KROUTILOVÁ, PHD.

ING. MILOSLAV STEINBAUER, PHD.

ING. MICHAL HADINEC

DOC. ING. PAVEL FIALA, PHD.

DOC. ING. KAREL BARTUŠEK, DRSC.

**Abstract:** This article deals with the verification of experimental results obtained by numerical simulation. We solved the effect of changes in the homogeneity of magnetic fields evoked by different samples from conductive and/or magnetic materials and the different types of inhomogeneity in the MR tomograph. Moreover, the paper will describe the suitable magnetic resonance techniques.

**Key words:** Inhomogeneity, numerical modelling, NMR

## 1 ANALYSIS OF THE TASK

The numerical modelling was realized using the finite element method together with the Ansys system. As the boundary condition, there was set the scalar magnetic potential  $\varphi_m$  by solving Laplace's equation

$$\Delta \varphi_m = \text{div } \mu (-\text{grad } \varphi_m) = 0 \quad (1)$$

together with the Dirichlet boundary condition

$$\varphi_m = \text{konst.} \quad (2)$$

on the areas  $\Gamma_1$  a  $\Gamma_2$ .

and the Neumann boundary condition

$$\mathbf{u}_n \cdot \text{grad } \varphi_m = 0 \quad (3)$$

on the areas  $\Gamma_3$  a  $\Gamma_4$ .

The continuity of tangential elements of the magnetic field intensity on the interface of the sample region is formulated by the expression

$$\mathbf{u}_n \times \text{grad } \varphi_m = 0 \quad (4)$$

The description of the quasi-stationary model MKP is based on the reduced Maxwell's equations

$$\text{rot } \mathbf{H} = \mathbf{J} \quad (5)$$

$$\text{div } \mathbf{B} = 0 \quad (6)$$

where  $\mathbf{H}$  is the magnetic field intensity vector,  $\mathbf{B}$  is the magnetic field induction vector,  $\mathbf{J}$  is the current density vector. For the case of the static magnetic irrotational field, the equation (5) is reduced to the expression (7).

$$\text{rot } \mathbf{H} = 0 \quad (7)$$

Material relations are represented by the equation

$$\mathbf{B} = \mu_0 \mu_r \mathbf{H} \quad (8)$$

where  $\mu_0$  is the permeability of vacuum,  $\mu_r(\mathbf{B})$  is the relative permeability of ferromagnetic material. The closed area  $\Omega$ , which will be applied for solving the equations (6) and (7), is divided into the region of the sample  $\Omega_1$  and the region of the medium  $\Omega_2$ . For these, there holds  $\Omega = \Omega_1 \cup \Omega_2$ . For the magnetic field intensity  $\mathbf{H}$  in area  $\Omega$  there holds the relation (7). The magnetic field distribution from the winding is expressed with the help of the Biot-Savart law, which is formulated as

$$\mathbf{T} = \frac{1}{4\pi} \int_{\Omega} \frac{\mathbf{J} \times \mathbf{R}}{|\mathbf{R}|^3} d\Omega \quad (9)$$

where  $\mathbf{R}$  is the distance between a point in which the magnetic field intensity  $\mathbf{T}$  is looked for and a point where the current density  $\mathbf{J}$  is assumed. The magnetic field intensity  $\mathbf{H}$  in the area can be expressed as

$$\mathbf{H}=\mathbf{T}-\text{grad } \phi_m \quad (10)$$

where  $\mathbf{T}$  is the preceding or estimated magnetic field intensity,  $\phi_m$  is the magnetic scalar potential. The boundary conditions are written as

$$\mathbf{u}_n \cdot \mu(\mathbf{T}-\text{grad } \phi_m)=0 \quad (11)$$

on the areas  $\Gamma_3$  and  $\Gamma_4$ .

where  $\mathbf{u}_n$  is the normal vector,  $\Gamma_{\text{Fe-0}}$  is the interface between the areas  $\Omega_{\text{Fe}}$  and  $\Omega_0 \cup \Omega_{\text{W}}$ . The area  $\Omega_0$  is the region of air in the model, the area  $\Omega_{\text{W}}$  is the region with the winding. The continuity of tangential elements of the magnetic field intensity on the interface of the area with ferromagnetic material is expressed

$$\mathbf{u}_n \times (\mathbf{T}-\text{grad } \phi_m)=0 \quad (12)$$

By applying the relation (10) in the relation (11) we get the expression

$$\text{div } \mu_0 \mu_r \mathbf{T}-\text{div } \mu_0 \mu_r \text{grad } \phi_m=0 \quad (13)$$

The equation can be discretized (13) by means of approximating the scalar magnetic potential

$$\phi_m = \sum_{j=1}^{NN} \varphi_j W_j(x, y, z) \quad (14)$$

$$\text{pro } \forall (x, y, z) \in \Omega$$

where  $\varphi_j$  is the value of the scalar magnetic potential in the  $j$ -th node,  $W_j$  the approximation function,  $NN$  the number of nodes of the discretization mesh. By applying the approximation (14) in the relation (13) and minimizing the residues according to the Galerkin method, we get the semidiscrete solution

$$\sum_{j=1}^{NN} \varphi_j \int_{\Omega} \mu \text{grad } W_i \cdot \text{grad } W_j \, d\Omega = 0, \quad (15)$$

$$i = 1, \dots, NN$$

## 2 GEOMETRICAL MODEL

Fig. 1 describes the sample geometry for the numerical modeling. On both sides, the sample is surrounded by the referential medium. During the real experiment, the reference is represented by water, which is ideal for obtaining the MR signal. As shown in fig. 1, in the model there are defined four volumes with different susceptibilities. The materials are defined by their permeabilities : material No. 1 – the medium outside the cube (air),  $\chi=0$ , material No. 2 – the inhomogeneous sample, (clay), material No. 3 - the material of inhomogeneities inside the sample. The permeability rate was set with the help of the relation  $\mu=1+\chi$ .

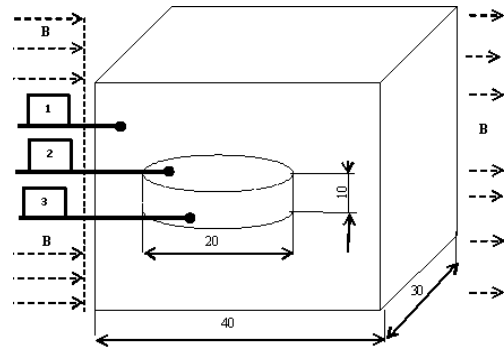


**Fig. 1** The sample geometry for numerical modeling

For the sample geometry according to fig. 1, the geometrical model was built in the system. In the model there was applied the mesh of elements, type Solid96 (Ansys). The boundary conditions (16) were selected for the induction value of the static elementary field to be  $B_0 = 4,7000$  T in the direction of the  $z$  coordinate (the cube axis) – corresponds with the real experiment carried out using the MR tomograph at the Institute of Scientific Instruments, ASCR Brno.

## 3. NUMERICAL ANALYSIS

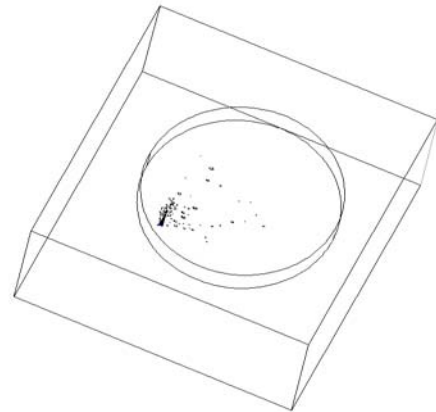


**Fig. 2** The geometrical model in the system

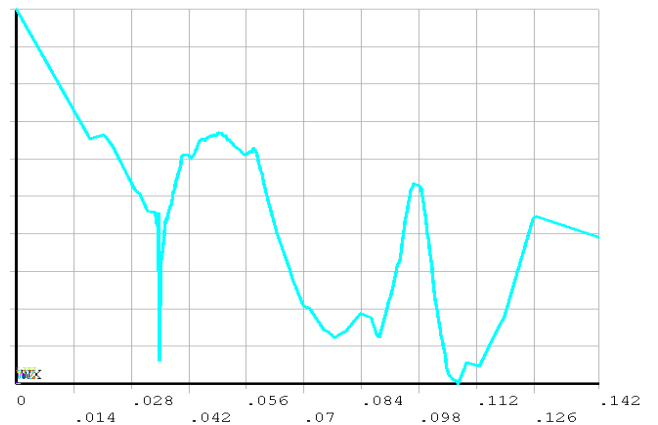


**Fig.3.** The distribution of the magnetic induction module in the section of the sample for material with  $\chi_m = -8,79 \cdot 10^{-6}$

The numerical modeling results are represented in fig. 3. The numerical modeling results were then used for the representation of the module of magnetic induction  $B$  along the defined path. For the model meshing, the element size selected as optimum was  $0,5 \cdot 10^{-3} \text{m}$ . The boundary conditions  $\pm\varphi/2$  were set to the model edges, to the external left and right boundaries of the air medium, as represented in fig.1. The excitation value  $\pm\varphi/2$  was set using again the relation (19). This is derived for the assumption that, in the entire area, there are no exciting currents, therefore there holds for the rot  $H = 0$  and the field is irrotational. Consequently, for the scalar magnetic potential  $\varphi_m$  holds

$$H = -\text{grad}\varphi_m \quad (16)$$

The potential of the exciting static field with intensity  $H_0$  is by applying (17)

$$\varphi_m = \int \vec{H}_0 \cdot \vec{u}_z dz = H_0 \cdot z \quad (17)$$

where

$$H_0 = \frac{B}{\mu_0 \cdot \mu_r} \quad (18)$$

Then

$$\pm \frac{\varphi}{2} = \frac{B \cdot z}{2\mu_0} = \frac{4,7000 \text{ T} \cdot 90 \text{ mm}}{2\mu_0} \quad (19)$$

where  $z$  is the total length of the model edge.

### 3 CONCLUSIONS

The experimental measuring was realized using the MR tomograph at the Institute of Scientific Instruments, ASCR Brno.

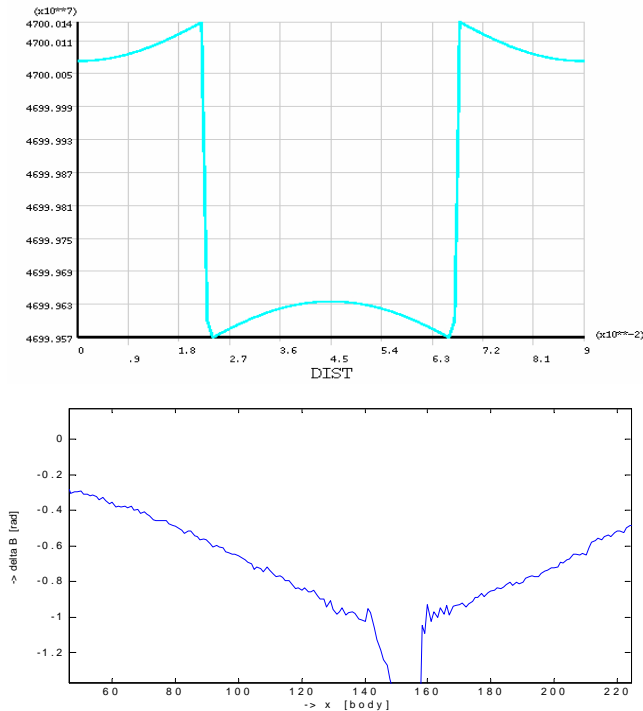


**Fig. 4** The measured pattern of magnetic induction  $B$ , through the medium, without the Hample

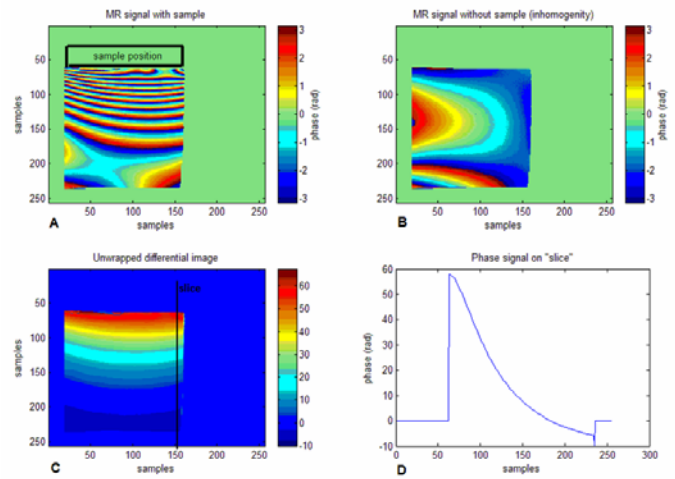


**Fig 5** The measured patterns for the inhomogeneous sample, clay

The tomograph elementary field  $B_0 = 4,7000 \text{ T}$  is generated by the superconductive solenoidal horizontal magnet produced by the Magnex Scientific company. The corresponding resonance frequency for the  $1\text{H}$  cores is  $200 \text{ MHz}$ . The numerical modeling and analysis of the task have verified the experimental results and, owing to the modifiability of the numerical model, we have managed to advance further in the experimental qualitative NMR image processing realized at the ISI ASCR

### ACKNOWLEDGEMENT

The research described in the paper was financially supported by research plans GAAV B208130603, MSM 0021630516 and GA102/07/0389.

### REFERENCES

- [1] Ansys User's Manual. Huston (USA): SVANSON ANALYSYS SYSTEM, Inc., 1994-2006.
- [2] Fiala, P., Kroutilová, E., Bachorec, T. Modelování elektromagnetických polí, počítačová cvičení. vyd. Brno: VUT v Brně, FEKT, Údolní 53, 602 00, Brno, 2005. s. 1 - 69 .
- [3] Steinbauer, M. Měření magnetické susceptibilitý technikami tomografie magnetické rezonance. vyd. Brno: VUT v Brně, FEKT, Údolní 53, 602 00, Brno, 2006.

Assoc. Prof. Pavel Fiala, Ph.D., Ing. Eva Kroutilova, Ph.D., Ing. Miloslav Steinbauer, Ph.D., Ing. Michal Hadinec, email fialap@feec.vutbr.cz, kroutila@feec.vutbr.cz, steinbau@feec.vutbr.cz, xhadin00@stud.feec.vutbr.cz  
Brno University of Technology, Faculty of Electrical Engineering and Communication, Department of Theoretical and Experimental Electrical Engineering, Kolejni 2906/4, 612 00 Brno  
Assoc. Prof. Ing. Karel Bartusek, CSc.  
Academy of Sciences of the Czech Republic, Institute of Scientific Instruments, Kralovopolska 147, 612 64 Brno, Czech Republic